ELSEVIER

Journal of Alloys and Compounds 446–447 (2007) 583–587

Journal of ALLOYS AND COMPOUNDS

www.elsevier.com/locate/jallcom

Hydrogen interactions with the PdCu ordered B2 alloy

S.M. Opalka [a,*], W. Huang [b], D. Wang [c], T.B. Flanagan [c], O.M. Løvvik [d,e], S.C. Emerson [a], Y. She [a], T.H. Vanderspurt [a]

[a] *United Technologies Research Center, 411 Silver Lane, East Hartford, CT 06108, United States*
[b] *QuesTek Innovations LLC, 1820 Ridge Avenue, Evanston, IL 60201, United States*
[c] *Department of Chemistry, University of Vermont, Burlington, VT 05405, United States*
[d] *University of Oslo, Centre for Materials Science and Nanotechnology, P.O.B. 1126 Blindern, NO-0318 Oslo, Norway*
[e] *Institute for Energy Technology, P.O.B. 40, NO-2027 Kjeller, Norway*

Received 24 October 2006; received in revised form 19 January 2007; accepted 22 January 2007
Available online 30 January 2007

Abstract

Combined experimental and modeling studies on hydrogen interactions with PdCu ordered body-centered cubic (B2) alloys have set the stage for membrane alloy development for advanced water gas shift membrane reactors that separate pure hydrogen from coal gasifier exhaust or syngas. First principles potential energy surface and ground state minimization calculations were used to profile the surface site selectivity of H_2 and H_2S adsorption on the lowest energy PdCu B2 (1 1 0) surface. Finite temperature surface energy calculations for varying H_2 and H_2S coverages were used to estimate the potential for blocking of H_2 adsorption by H_2S physisorption under coal gasification partial pressure and temperature conditions. Experimental measurements of hydrogen solubility in the $Pd_{0.44}Cu_{0.56}$ B2 alloy were made with a Sievert's type apparatus. This data was assessed, along with existing experimental data and first principles predicted finite temperature data for hypothetical end-member phases, to develop a thermodynamic description of the ternary Pd–Cu–H system encompassing the PdCu B2 phase. First principles ground state and lattice dynamics simulations were used to predict favorable pathways for thermally activated hydrogen diffusion within the B2 lattice. The newly derived solubility and diffusivity parameters were evaluated within a mass transfer model to predict the ideal bulk permeability in the absence of other mass transfer contributions.

Keywords: Metals and alloys; Hydrogen adsorbing materials; Phonons; Diffusion; Thermodynamic modeling

1. Introduction

Advanced water gas shift membrane reactors (AWGSMR) use hydrogen-selective membranes to increase the conversion of coal or natural gas-derived syngas to H_2 by the heterogeneously catalyzed water gas shift (WGS) reaction, $CO + H_2O \leftrightarrows CO_2 + H_2$ ($\Delta H_{reaction} = -41$ kJ/mol). The exothermic WGS reaction is kinetically controlled at low temperatures and thermodynamic equilibrium-controlled at high temperatures. The use of a membrane to continuously remove the H_2 product increases the conversion rate at high temperatures, shifting the reaction towards completion. The AWGSMR path to low cost H_2 production eliminates the need for multi-stage WGS reactors with intermediate cooling, carbon oxide cleanup units, and pressure swing adsorption units, resulting in a single stage, simpler process with less catalyst and lower reactor volume, in addition to providing high purity H_2.

This technology requires a thin noble metal alloy membrane to selectively permeate H with low mass transfer resistance in the presence of competitive WGS co-reactants and contaminants, especially hydrogen sulfide, H_2S, and related sulfur-species. The development of crack-free, high H-selectivity membranes that are stable to thermal and pressure cycling and resistant to the poisoning of surface H_2 adsorption and dissociation sites, is an active area of research. It has been shown that below 350 °C, the $Pd_{0.47}Cu_{0.53}$ ordered body-centered cubic (B2) alloy has a high H permeability and a reported tolerance to H_2S [1]. However, implementation of this membrane alloy presents some challenges. The Pd–Cu binary phase diagram in Fig. 1 shows that while this composition occurs within the single B2 phase

* Corresponding author. Tel.: +1 860 610 7195; fax: +1 860 610 1661.
E-mail address: opalkasm@utrc.utc.com (S.M. Opalka).

0925-8388/$ – see front matter © 2007 Elsevier B.V. All rights reserved.
doi:10.1016/j.jallcom.2007.01.130

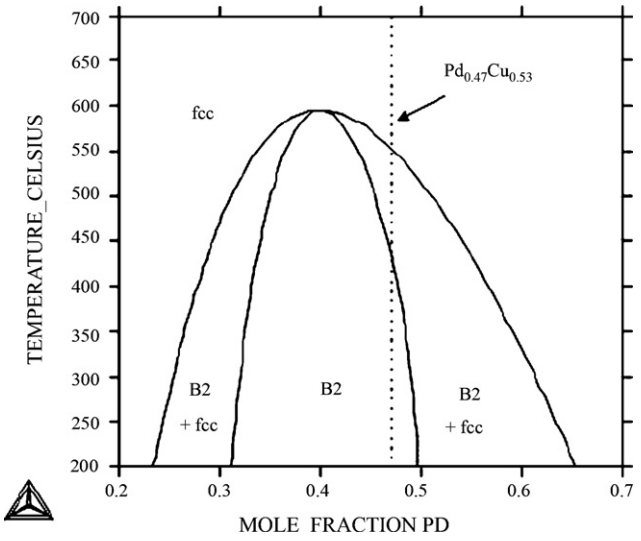

Fig. 1. Pd–Cu phase diagram developed by thermodynamic modeling, with dashed line showing placement of the high permeability $Pd_{0.47}Cu_{0.53}$ composition.

region with a maximum at 40 at.% Pd and 596 °C, it is perilously close to the B2 + fcc phase boundary on the low Cu side. This single phase composition may not be stable upon thermal cycling to higher temperatures, such as up to 450 °C, that may be required for operation of a WGS membrane reactor. It is also anticipated that the selective adsorption of co-reactants such as carbon monoxide or sulfur-species could possibly induce preferential surface segregation of Cu, thereby shifting the composition outside of the single B2 phase region [2]. The formation of the fcc phase with a different molar volume could compromise the integrity and H-selectivity of the membrane. Moreover, the fcc phase that surrounds the B2 single phase region has a significantly lower H permeability compared to the B2 phase.

This study investigated surface reactions, H diffusion, and membrane performance in the PdCu ordered B2 alloy [3–9], to develop a comprehensive description of H permeation in $Pd_{(1-x)}Cu_x$ B2 alloys formed over the intermediate Pd–Cu composition range. This description will serve to benchmark the behavior of the PdCu B2 alloys and to set the stage for developing new alloys with improved thermal and chemical stability and uncompromised H permeability performance. Mechanisms for H_2 adsorption, dissociation, and solubilization on the PdCu (1 1 0) surface will be proposed from first principles (FP) simulations. This understanding will be used to predict the surface contributions to H absorption under temperatures and pressures, including >1 ppm partial pressure of H_2S relevant to AWGSMR operation on syngas. A thermodynamic description of the Pd–Cu–H system is presented that is based on the newly developed descriptions of the Pd–Cu, Pd–H and Cu–H binary systems, available ternary experimental data from the literature, new experimental measurements of H solubility in the B2 phase, and FP predicted stabilities of related B2 compounds. This description enabled the calculation of phase stability and H solubility within this phase region over a wide range of temperatures and pressures. FP lattice dynamics were used to simulate and parameterize dilute H thermally activated interstitial diffusion within the PdCu B2 lattice. The modeled H solubility and diffusivity parameters were used to predict the ideal bulk H permeability.

2. Methodology

The periodic atomic structures of known and hypothetical bulk phases in the Pd–Cu–H system were predicted with the density functional theory Vienna ab initio simulation package (VASP) code [10,11] full minimizations using hard Pd_pv $4p^6$ $4d^{10}$, hard Cu_pv $3p^6$ $3d^{10}$ $4s^1$, and the regular H $1s^1$ projector augmented wave potentials [12] with the generalized gradient PW91 exchange-correlation corrections [13], 0.3 $Å^{-1}$ or finer spacing of the **k**-point meshes, and spin polarization. The low energy (1 1 0) surface of the stoichiometric PdCu composition was selected to represent surface reactions on the ordered B2 phases. All calculations were made with a planewave cutoff of 410 eV and Methfessel Paxton smearing using a broadening of 0.5 eV. The criteria for convergence of the atomic forces in the bulk and slab relaxations were 0.005 eV/Å. The thermodynamic properties of selected relaxed phases were predicted with direct method lattice dynamics using the Materials Design MedeA Phonon module [14,15] using the harmonic approximation with 0.002 Å one-sided displacements of symmetry unique atoms. Thermodynamic property predictions were determined from the integration of the vibrational density of states over the entire Brillouin zone. The lattice dynamics of dilute interstitial and transition state H interactions were simulated in a $2 \times 2 \times 2$ PdCu B2 supercell allowing only initial minimization of atomic positions.

The adsorptive interactions of H_2, H and H_2S were simulated on one side of a 32 atom 4 layer periodic PdCu B2 (1 1 0) slab separated by 10 Å vacuum, using a $3 \times 3 \times 1$ Monkhorst-Pack **k**-point mesh without spin polarization. Potential energy surfaces (PES) were determined from 0.25 H_2S and H_2 monolayer (ML) single point calculations made with the adsorbates at progressively spaced distances above selected PdCu (1 1 0) representative surface sites. Ionic relaxations were made to evaluate the 0.25–1.0 ML H_2 and H_2S adsorption configurations, fixing only the bottom atomic layer. These results were used to estimate the surface energies of PdCu (1 1 0) surfaces with varying coverages of adsorbed H_2 and H_2S at AWGSMR reactor temperatures and partial pressures, based on the method of Arrouvel et al. [16], which approximates temperature and pressure contributions with the chemical potential of the adsorbate gas phase and does not describe the vibrational or configurational contributions of the adsorbate-condensed phases.

Thermodynamic descriptions were recently developed for the Pd–Cu, Pd–H, and Cu–H binary, and the Pd–Cu–H ternary systems [17]. A literature review was made to identify relevant experimental phase equilibrium and thermochemical data. Hydrogen solubility measurements were made on a $Pd_{0.44}Cu_{0.56}$ B2 alloy using a Sievert's apparatus over the 100–350 °C temperature range [17]. The thermodynamic properties were analyzed using thermodynamic models for the Gibbs energy of the individual phases. The model parameters were optimized using selected experimental and theoretical data. Discrepancies among

experimental data of various types and sources were detected during the optimization, and the weighting of selected experimental data was adjusted accordingly. The thermodynamic description thus obtained was self-consistent, enabling phase diagram modeling for a wide range of compositions, temperatures, and pressures.

3. Results and discussion

It is clear from the literature that H_2S and S contaminant species significantly poison the H permeability of PdCu membranes [2,7,9]. In order to understand these competitive mechanisms, PES calculations and ground state minimizations were made to profile the interactions of H_2, H, and H_2S with representative PdCu (1 1 0) surface sites. In the most stable relaxed ground state adsorption configuration, one H_2 molecule on a 4×4 PdCu (1 1 0) slab [0.25 monolayer (ML)] adsorbs 1.9 Å above a surface Pd atom with the molecular axis parallel to the surface, binding with a −28.64 kJ/mol per H_2 modest favorable energy. There is negligible change in energy with rotation of the H_2 horizontal alignment. In the full H_2 monolayer the adsorption energy decreases to −21.4 kJ/mol per H_2 and the H_2 molecules orient towards the nearest neighbor subsurface Pd atoms. A reaction pathway was established for H_2 dissociation leading to adsorption of the two H atoms on adjacent four-fold hollow surface sites centered above subsurface Cu atoms, displaced 0.6 Å from the hollow center in the [1 0 0] direction. In the optimum 0.25 ML H configuration, the Pd–H distance is 0.8 Å and the binding energy is −50.0 kJ/mol per H atom. In the most favorable relaxed 0.25 ML H_2S configuration, the S atom adsorbs 2.4 Å above a surface Pd atom with the molecular plane tilted 16° away from the surface plane with a strong binding energy of −70.9 kJ/mol, in good agreement with previous work [3]. In the 1.0 ML adsorbed H_2S configuration, the H_2S molecules rotate alternately in opposite directions to minimize repulsion and facilitate hydrogen-bonding with a significantly reduced binding energy. Repulsive interactions at high ML fractions could facilitate H_2S dissociative adsorption, leading to sulfur surface poisoning shown to be very favorable by atomic simulations [4]. The adsorption of H_2 and H_2S on adjacent surface Pd atoms has a combined reduced binding energy of −77.2 kJ/mol, most likely due to the poisoning interactions of the adsorbed H_2S. Finite temperature surface energy predictions were made for coal gasification feed H_2 and H_2S partial pressures of 2×10^{-2} and 3×10^{-6} bar, respectively. The predictions showed that at these partial pressures, H_2 physisorption of up to 0.5 ML coverage would be favorable at the 673 K reactor operating temperature without the interference of H_2S site blocking. Hydrogen sulfide is predicted to only remain physisorbed in a 0.25 ML coverage up to 430 K. These predictions do not take the contributions from irreversible H_2S dissociative adsorption into account.

The calculated fcc and B2 phase equilibria from the newly established thermodynamic description of the Pd–Cu system [17] is shown in Fig. 1. The Pd–Cu solid phase boundaries do not vary appreciably with pressure and the phase descriptions are pressure independent. The FP finite temperature predictive capability was validated by showing acceptable agreement

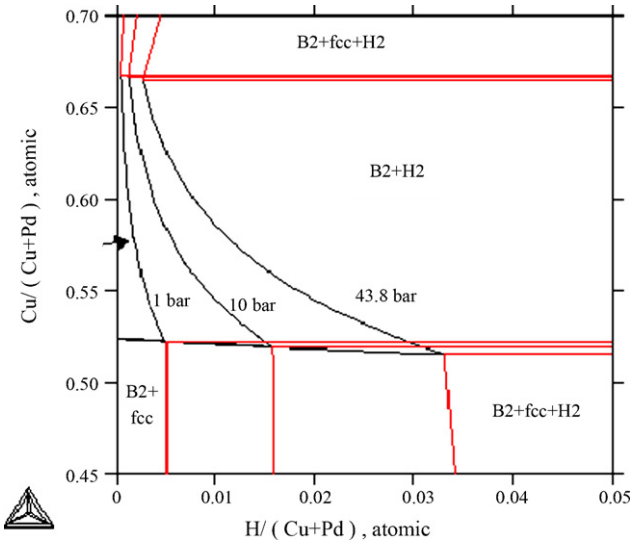

Fig. 2. Calculated H solubility in the PdCu B2 phase at 673 K (400 °C) over a range of pressures, up to 43.8 bar (WGS reactor operating conditions).

between the FP predicted and thermodynamically modeled Gibbs free energies of formation, $\Delta G_{form}(T)$, for the $Pd_{0.5}Cu_{0.5}$ and $Pd_{0.4}Cu_{0.6}$ B2 compositions, the differences being well within 5 kJ/mol up to 1000 K. The Pd–Cu–H thermodynamic description was collectively developed from newly obtained $Pd_{0.44}Cu_{0.56}$ B2 H solubility data, established experimental data for H_2 desorption isotherms, para-equilibrium miscibility gap boundaries, and partial H enthalpies for Pd–Cu–H fcc alloys with up to 30 at.% Cu, and from FP predictions of the thermodynamic stability of the B2 alloys [17]. The thermodynamic modeling enabled the prediction of H solubility in the B2 phase over a wide range of temperatures and pressures, for example, as shown in Fig. 2 for several different pressures up to 43.8 bar H_2 pressure at the 673 K (400 °C) temperature for AWGSMR operation. Absorbed H slightly shifts both B2 phase boundaries towards lower Cu concentrations, where the shifts increase with H_2 pressure. The H solubility is at a maximum on the low Cu side of the B2 phase, exhibiting a maximum ratio of 0.033 H/metal (3.2 at.%) at the $Pd_{0.48}Cu_{0.52}$ composition at the 43.8 bar and 673 K operating conditions. Thus, the high permeability $Pd_{0.47}Cu_{0.53}$ composition was predicted to be stable in the B2 form and to have near optimum H solubility for AWGSMR operation.

To benchmark our atomic modeling capability for FP H diffusivity predictions, the interstitial solubility and movement of atomic H was simulated within a $2 \times 2 \times 2$ supercell of an ordered $Pd_{0.50}Cu_{0.50}$ B2 composition (model stoichiometry = Pd_8Cu_8H). The PdCu stoichiometry was used to approximate the high permeability $Pd_{0.47}Cu_{0.53}$ ordered B2 composition with a reasonable level of computational resources. This model H concentration (H/M = 0.0625) is well above the solubility limits determined from our thermodynamic modeling, and would undergo a 3 $Å^3$ unit cell volume expansion during ground state full minimization, which correlates well with established experimental relationships [18]. In order to realistically represent a more dilute concentration regime, the PdCu

lattice was fixed and only ionic relaxation was allowed during the interstitial H substitution simulations. At the ground state, the tetrahedral site bounded by two Pd and two Cu atoms was found to be slightly more energetically favorable (−2.52 kJ/mol) than the octahedral site bounded by four Pd and two Cu atoms. Lattice dynamic calculations were made with the direct method including the phonon interactions of all the lattice ions with the H atom in the interstitial and transition states, and to confirm the identity of the transition state. The Pd_4Cu_2 octahedral site with H exhibited two nearly equivalent imaginary frequencies atypical of a saddlepoint, and was not considered to be part of the stable H migration pathway. The lowest activation barrier, ΔH_{act}, for the multiple diffusion pathways examined within the frozen atomic lattice was found to be from diffusion between tetrahedral sites through a Pd_2Cu triangular face. This diffusion pathway was reported in an earlier study allowing full bulk minimization of H solubilized in the PdCu lattice [5], however, it was refuted in a later study with the same co-authors [6]. The zero point energy (ZPE) corrections for H in the tetrahedral site and in the transition state were determined from the real H vibrational frequencies predicted at the gamma point. The ZPE-corrected activation barrier [$\Delta H_{act} + \Delta ZPE_H$], was 6.96 kJ/mol, compared to ∼2 kJ/mol activation barrier reported for comparable fully minimized structures [5]. Following the approach of Jiang and Carter [19], the quantum-corrected diffusion equation:

$$D = \left[\frac{n\alpha^2\kappa_B T}{6h}\right] \exp\left[\frac{-\Delta H_{act} + \Delta ZPE_H}{\kappa_B T}\right] \quad (1)$$

where n is the geometrical jump factor, α the tetrahedral-to-tetrahedral jump length of 1.5 Å, κ_B the Boltzmann's constant, and h is the Planck's constant, was used to determine a preexponential factor, D_0, of 2.1×10^{-7} m^2/s and a diffusivity, D, of 6.3×10^{-8} m^2/s at 673 K (400 °C). Fig. 3 shows that there is reasonable agreement between the FP predicted H diffusivity in $Pd_{0.5}Cu_{0.5}$ and that measured in the $Pd_{0.47}Cu_{0.53}$ B2 by Piper [20] and Völkl and Alefeld [21]. The latter data set was also included the measured $Pd_{0.47}Cu_{0.53}$ face-centered cubic alloy diffusivity for comparison.

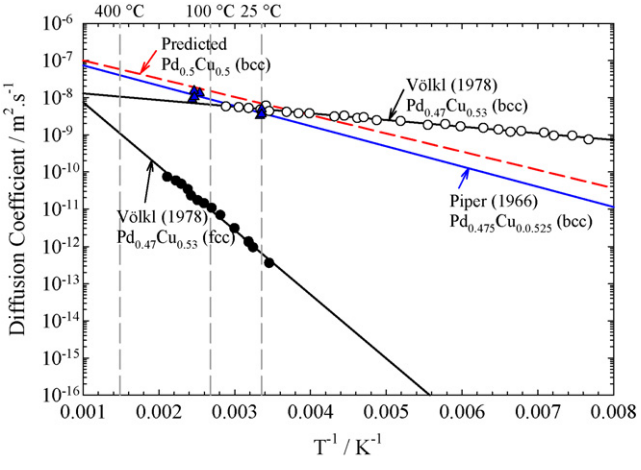

Fig. 3. Comparison of predicted H diffusivities coefficients to literature experimental data from Piper [20] and Völkl and Alefeld [21].

The prediction of the ideal H permeability, Q (in units of mol s^{-1} m^{-1} Pa$^{-0.5}$), the product of solubility and diffusivity for a given alloy, enables the quantitative evaluation of surface contributions in experimental permeability data. In a one-dimensional membrane mass transfer model, the H flux, J_{H_2}, is given by

$$J_{H_2} = \left(\frac{Q}{\ell}\right)(p_1^{0.5} - p_2^{0.5}) = \left(\frac{D}{\ell}\right)(C_1 - C_2) \quad (2)$$

where ℓ is the membrane thickness, p_1 and p_2 are the H_2 partial pressures above the membrane surface, C_1 and C_2 are the surface soluble H concentrations in mol/m^3, and where the subscripts 1 and 2 refer to the retentate and permeate sides of the membrane [22]. The surface H concentration, C, is proportional to the H/metal ratio, n, by κ, a conversion factor (in units of mol H/m^3) corresponding to the lattice volume when $n = 1$, where n is proportional to the square root of pressure, $p^{0.5}$, by Sievert's constant, K_s. Using these relationships, J_{H_2} can be expressed as

$$J_{H_2} = (D\kappa K_s)(\ell)^{-1}(p_1^{0.5} - p_2^{0.5}) \quad (3)$$

The solubility can therefore be determined from the product [κK_s]. The kappa conversion factor, κ, for the lattice volume when $n = 1$, was estimated from the $Pd_{0.47}Cu_{0.53}$ lattice and the established H partial molar volume increase relationship for Pd alloys [18], to be 1.0×10^5 mol H/m^3. Hydrogen solubility in $Pd_{0.47}Cu_{0.53}$ was calculated from the Pd–Cu–H thermodynamic assessment modeling [17], where the Sievert's coefficient, K_s, is determined from the inverse slope of the square root of H_2 pressure versus the solubilized H/(Pd + Cu) metal ratio. The calculated solubility plot for $Pd_{0.47}Cu_{0.53}$ at 673 K is shown in Fig. 2, where K_s was determined to be 1.25×10^{-5} Pa$^{-0.5}$. Using the FP calculated diffusivity, the estimated κ conversion factor, and the K_s Sievert's coefficient from the thermodynamic assessment, the theoretical H bulk permeability, Q, was estimated to be 7.9×10^{-8} mol s^{-1} m^{-1} Pa$^{-0.5}$ in $Pd_{0.47}Cu_{0.53}$ at 673 K. Most experimental $Pd_{0.47}Cu_{0.53}$ membrane results are reported in terms of permeance for membranes of varying thickness and configuration, making direct comparison difficult. Our predicted permeability is more than an order magnitude larger than the permeabilities predicted and measured by Kamakoti et al. [6], however, it is consistent with the report that H permeability of the $Pd_{0.47}Cu_{0.53}$ B2 phase is 1.1 times larger than Pd at 623 K [23]. We plan to conduct experiments to validate our modeling, using an experimental configuration and mass transfer model that eliminates other mass transfer contributions to the determination of bulk permeability.

4. Conclusion

Atomic–thermodynamic modeling, experimental H solubility measurements, and thermodynamic assessments were used to investigate H adsorption, solubility, and diffusion in PdCu ordered B2 alloys. Without taking irreversible dissociative H_2S adsorption into account, preliminary surface energy predictions show that H_2 adsorption is not significantly poisoned by H_2S physisorption under AWGSMR temperatures,

pressures, and H_2S concentrations projected for coal gasification. First principles diffusivity predictions based on direct method lattice dynamics, H solubility measurements, and thermodynamic assessments were used to collectively predict the H permeability in bulk PdCu in the absence of surface contributions.

Acknowledgements

S.M. Opalka, S.C. Emerson, Y. She, and T.H. Vanderspurt gratefully acknowledge the support by US DOE Contract DE-FG26-05NT42453. O.M. Løvvik acknowledges support from the Norwegian Research Council through the Nanomat program. Helpful discussions were held with Paul Saxe of Materials Design, Inc. and Greg B. Olson of QuesTek Innovations LLC.

References

[1] F. Roa, M.J. Block, J.D. Way, Desalination 147 (2002) 411.
[2] H. Gao, Y.S. Lin, Y.D. Li, B.Q. Zhang, Ind. Eng. Chem. Res. 43 (22) (2004) 6920.
[3] D.R. Alfonso, A.V. Cugini, D. Sorescu, Prepr. Pap. Am. Chem. Soc. Div. Fuel Chem. 48 (2) (2003) 512.
[4] D.R. Alfonso, A.V. Cugini, D.S. Sholl, Surf. Sci. 546 (1) (2003) 12.
[5] P. Kamakoti, D.S. Sholl, J. Membr. Sci. 225 (2003) 145.
[6] P. Kamakoti, B.D. Morreale, M.V. Ciocco, B.H. Howard, R.P. Killmeyer, A.V. Cugini, D.S. Sholl, Science 307 (2005) 569.
[7] B.D. Morreale, M.V. Ciocco, B.H. Howard, R.P. Killmeyer, A.V. Cugini, R.M. Enick, J. Membr. Sci. 241 (2004) 219.
[8] A. Kulprathipanja, G.O. Alptekin, J.L. Falconer, J.D. Way, Ind. Eng. Chem. Res. 43 (2004) 4188.
[9] A. Kulprathipanja, G.O. Alptekin, J.L. Falconer, J.D. Way, J. Membr. Sci. 254 (2005) 49.
[10] G. Kresse, J. Hafner, Phys. Rev. B 47 (1) (1993) 558.
[11] G. Kresse, J. Furthmüller, Comput. Mater. Sci. 6 (1996) 15.
[12] G. Kresse, D. Joubert, Phys. Rev. B 59 (1999) 1758.
[13] J.P. Perdew, J.A. Chevary, S.H. Vosko, K.A. Jackson, M.R. Pederson, D.J. Singh, C. Fiolhais, Phys. Rev. B 46 (1992) 6671.
[14] K. Parlinski, Z.Q. Li, Y. Kawazoe, Phys. Rev. Lett. 78 (1997) 4063.
[15] MedeA-Phonon Version 1.0 using Phonon Software 4.24, Copyright Prof. K. Parlinski.
[16] C. Arrouvel, H. Toulhoat, M. Breysse, P. Raybaud, J. Catal. 226 (2) (2004) 260.
[17] W. Huang, S.M. Opalka, D. Wang, T.B. Flanagan, CALPHAD, accepted.
[18] The hydrogen partial molar volume increase has been determined to be 1.77×10^{-24} m^3/mol H from a number of binary Pd alloys, This relationship was first reported by B. Baranowski, S. Majchrzak, T.B. Flanagan, J. Phys. F 1 (1971) 258.
[19] D.E. Jiang, E.A. Carter, Phys. Rev. B 70 (2004) 064102.
[20] J. Piper, J. Appl. Phys. 37 (1966) 715.
[21] J. Völkl, G. Alefeld, Diffusion of hydrogen in metals, in: G. Alefeld, J. Völkl (Eds.), Hydrogen in Metals, vol. I, Springer-Verlag, Berlin, 1978, pp. 321–348 (vol. 28 of topics in Applied Physics).
[22] J. Shu, B.P.A. Grandjean, A. Van Neste, S. Kaliaguine, Can. J. Chem. Eng. 69 (1991) 1036.
[23] Y.H. Ma, E.E. Engwall, I.P. Mardilovich, Preprints of Symposia—American Chemical Society, Division of Fuel Chemistry 48 (1) (2003) 333.